ELSEVIER

Surface Science 369 (1996) 351–359

surface science

Atomic resolution STM imaging of electrochemically controlled reversible promoter dosing of catalysts

M. Makri [a], C.G. Vayenas [a,*], S. Bebelis [a], K.H. Besocke [b], C. Cavalca [c]

[a] *Department of Chemical Engineering, University of Patras, Patras GR-26500, Greece*
[b] *Besocke Delta Phi, Tuchbleiche 8, D-52428 Jülich, Germany*
[c] *Department of Chemical Engineering, Yale University, New Haven, CT 06520, USA*

Received 14 April 1996; accepted for publication 1 July 1996

Abstract

Reversible electrochemically controlled dosing (back-spillover) of sodium on Pt(111) at atmospheric pressure was imaged via atomically resolved STM. The Pt(111) monocrystal was interfaced with a flat polycrystalline sample of β''-Al_2O_3, a Na^+ conductor. Application of an electrical current between the Pt(111) monocrystal and a counterelectrode also in contact with the β''-Al_2O_3 Na^+-conducting solid electrolyte causes reversible migration (back-spillover and spillover) of sodium, which forms a (12×12) hexagonal structure on the Pt(111) surface. In addition to explaining the phenomenon of electrochemical promotion in heterogeneous catalysis, these observations provide the first STM confirmation of spillover phenomena which play a key role in numerous catalytic systems.

Keywords: Catalysis; Electrochemical methods; Metal–solid electrolyte interfaces; Platinum; Promotion; Scanning tunneling microscopy; Sodium; Surface diffusion

1. Introduction

Since the pioneering work of Rohrer and Binnig [1], scanning tunneling microscopy (STM) has been used to image atomic-scale features of conductive surfaces under ultra-high vacuum (UHV) [2–4], but also at atmospheric pressure [5] and in aqueous electrochemical environments [6–9]. The ability of STM to image surface reconstruction [10] and chemisorption [11] is well documented [12], and is of paramount importance in the fields of surface science [13] and heterogeneous catalysis [14].

In addition to reactant chemisorption and surface reconstruction, promotion also has a key role in heterogeneous catalysis [15–18]. Promoters are routinely used in most industrial heterogeneous catalytic systems at atmospheric or higher pressures, (e.g. K-promoted Fe catalysts used for ammonia synthesis [16]), yet their exact role is only well understood at the molecular level for a few model systems under UHV [17,18].

Spillover/back-spillover of reactants and products from/to catalytically active metal surfaces to/from oxide supports has been invoked to explain numerous observations in heterogeneous catalysis [19]. The evidence for spillover or back-spillover is usually indirect [19], and only recently has X-ray photoelectron spectroscopy (XPS) been used

* Corresponding author. Fax: +30 61 997269; e-mail: cat@rea.iceht.forth.gr

PII S0039-6028(96)00911-9

to show that oxygen spillover and back-spillover is a real phenomenon for some systems [20].

Back-spillover and spillover of promoting ions has also been proposed as the cause of the effect of non-Faradaic electrochemical modification of catalytic activity (NEMCA) [21] or electrochemical promotion [22,23], which has been reported recently for over 40 catalytic reactions [24]. It was found that the catalytic activity and selectivity of metals interfaced with solid electrolytes such as Y_2O_3-stabilized ZrO_2 (YSZ), an O^{2-} conductor, or β''-Al_2O_3, an Na^+ conductor, can be varied dramatically and reversibly by applying electric currents or potentials between the catalyst film and a counterelectrode also deposited on the solid electrolyte [21,22,24]. The increase in the rate of catalytic reactions is up to a factor of 3×10^5 higher than the rate of supply of ions to the catalyst electrode [24] and up to a factor of 100 [24,25] or higher [26] than the open-circuit (unpromoted) catalytic rate. The importance of electrochemical promotion in catalysis [16] and electrochemistry [27] has been discussed recently by Haber [16] and Bockris [27], respectively. Recent kinetic [21–25], work function [21,28], XPS [20,26,29], UPS [30], surface-enhanced Raman spectroscopic (SERS) [31,32], temperature-programmed desorption (TPD) [33] and cyclic voltammetric [24,33] studies have provided strong evidence that the effect of electrochemical promotion is due to electrochemically induced and controlled back-spillover of promoting ionic species from the solid electrolyte onto the catalyst surface. These ionic species ($O^{\delta-}$ in the case of YSZ, $Na^{\delta+}$ in the case of β''-Al_2O_3) form an "effective electrochemical double layer" on the gas-exposed catalyst-electrode surface [24,34] which affects the chemisorptive bond strength of coadsorbed reactants and intermediates [24,35], and thus causes very pronounced changes in catalyst activity.

In this work we show that, in addition to reactant chemisorption and surface reconstruction, STM can also be used to image promoters on metal catalyst surfaces under conditions relevant to catalysis. We also provide concrete STM evidence that both spillover and back-spillover are real phenomena over enormous distances (mm), and that electrochemically controlled back-spillover is the cause of electrochemical promotion in catalysis [21–24].

2. Experimental

Fig. 1 shows the sample geometry. The polished Pt(111) single crystal (10 mm × 10 mm × 1 mm) was mounted on the appropriately shaped surface of the polycrystalline β''-Al_2O_3 sample (20 mm × 20 mm × 3 mm). Good mechanical and electrical contact between the metal and the solid electrolyte was established by coating a thin (~10 μm) Au layer along the perimeter of the Pt/β''-Al_2O_3 contact. The Au layer was covered by a porous Pt film (thickness ~10 μm) similar to those used in electrochemical promotion experiments [21,22,24,25]. The Au and Pt films were prepared using thin coatings of unfluxed Au and Pt pastes followed by calcination at 850°C as described elsewhere [24]. This design permits the same type of interfacing between single-crystal metal surfaces and solid electrolyte components as that between polycrystalline metal films and solid electrolytes used in all previous electrochemical promotion experiments [21,22,24,28]. This electrical interfacing between the Pt single crystal and the solid electrolyte provides a significant extent of three-phase boundaries between the solid electrolyte, the metal catalyst-electrode and the gas phase. These three-phase boundaries contain the active sites for charge transfer reactions, e.g. for the transformation of Na^+ in β''-Al_2O_3 to $Na^{\delta+}$ adsorbed on the Pt surface upon negative current application [21,24].

Constant currents I between the Pt(111) single crystal and the Pt counterelectrode were applied via an AMEL 553 galvanostat while monitoring the Pt(111) potential V_{WR} with respect to the reference Pt electrode. The STM used in this work was a Besocke beetle-type [36] made by Besocke-Delta-Phi Electronic. The tunneling tips were mechanically etched 80mol%Pt–20mol%Rh wires (Longreach Scientific Research).

3. Results

Atomic resolution STM images of the ambient air-exposed Pt(111) surface before current

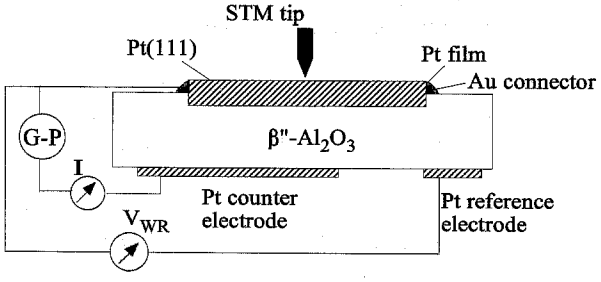

(a)

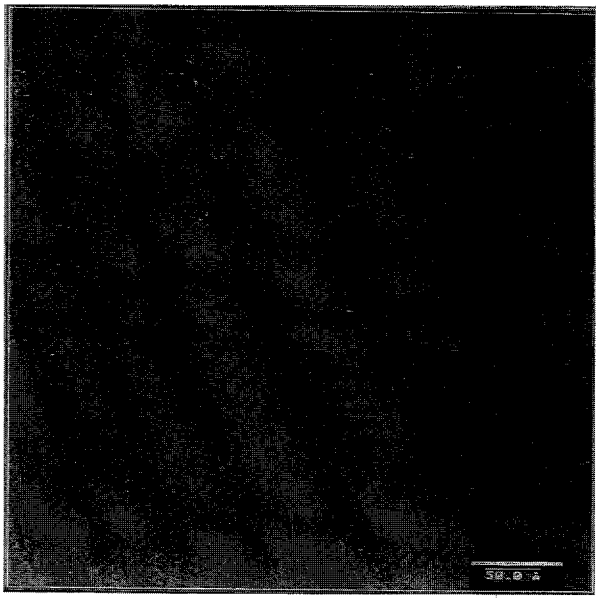

(b)

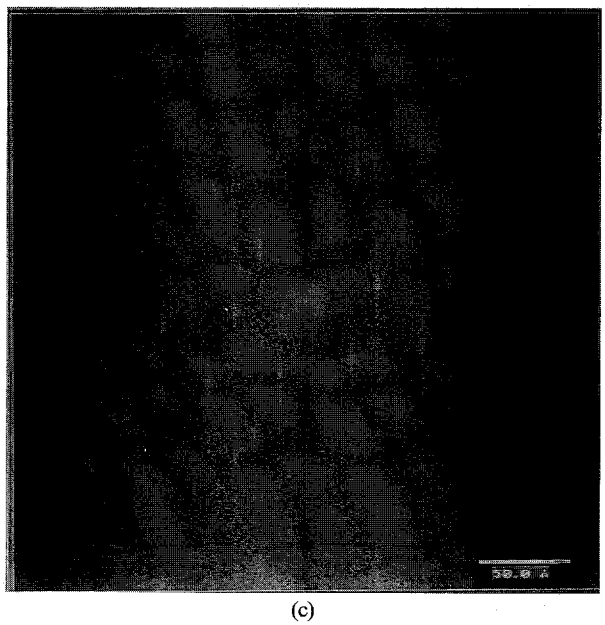

(c)

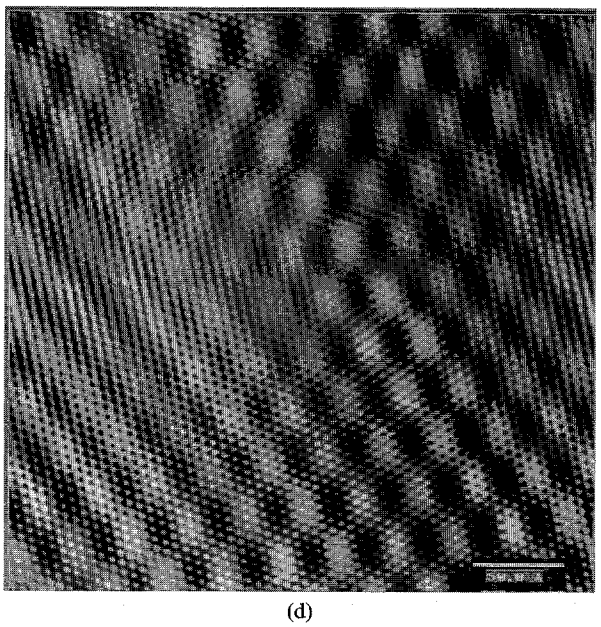

(d)

Fig. 1. (a) Experimental setup. (b) STM image (unfiltered) of the initially sodium-contaminated Pt(111)-(2×2)-O adlattice. (c) Corresponding Fourier transform spectrum. (d) Fourier-filtered STM image of the overlapping Pt(111)-(2×2)-O and Pt(111)-(12×12)-Na adlayers (V_t=80 mV, I_t=10 nA, total scan size 319 Å).

application showed the Pt(111)-(2×2)-O adlattice (interatomic distance 5.61 Å, Fig. 1b) and local patches of an overlapping Pt(111)-(12×12)-Na adlayer (interatomic distance 33.2 Å, Fig. 1b).

This second adlayer results from thermal diffu-

sion of sodium on the Pt(111) surface during the preparation of the connecting polycrystalline Pt film [22]. The presence of this second adlayer is also manifest by the dots near the centre of the corresponding two-dimensional Fourier transform spectrum (Fig. 1c). Fig. 1d shows the Fourier-filtered STM image of the overlapping Pt(111)-(2 × 2)-O and Pt(111)-(12 × 12)-Na adlayers.

Positive current application ($I = 1$ μA for $t = 360$ s at 550 K), corresponding to the electrochemical removal of $It/F = 3.7 \times 10^{-9}$ mol Na, and leading to a Pt(111) catalyst potential $V_{WR} = 0.4$ V with respect to the reference electrode, caused the disappearance of the Pt(111)-(12 × 12)-Na overlayer structure, leaving the Pt(111)-(2 × 2)-O adlattice intact (Fig. 2a). This shows that sodium spillover from the Pt(111) surface to the β''-Al_2O_3 solid electrolyte has taken place, and that the gas-exposed electrode surfaces of metals interfaced with solid electrolytes can be cleaned electrochemically as proposed previously [22,24].

Subsequent application of negative current ($I = -1$ μA for $t = 1400$ s at 550 K), corresponding to the electrochemical supply of $-It/F = 1.5 \times 10^{-8}$ mol Na and leading to a 1 V decrease in catalyst potential V_{WR}, and thus [21,24] a 1 eV decrease in the work function $e\Phi$ of the Pt(111) surface, caused the reappearance of the Pt(111)-(12 × 12)-Na overlayer structure everywhere on the Pt surface (Fig. 2b).

Figs. 3a and 3b show atomically resolved images of larger areas of the sodium-free (Fig. 3a) and sodium-doped (Fig. 3b) Pt(111) surface with the corresponding two-dimensional Fourier transform spectra. Both the unfiltered STM images and the Fourier transform spectra clearly show the reversible appearance and disappearance of the Pt(111)-(12 × 12)-Na structure. Smaller areas of the sodium-free and sodium doped Pt(111) surface are shown in Figs. 4a and 4b. It is worth noting that each Na atom appears to perturb the electron density of the Pt(111) surface over large (~12) atomic distances. This can explain the observed "long-range" promotional effect of Na on Pt surfaces [24] and is strongly reminiscent of the IR spectroscopic work of Yates and co-workers [37], who showed that a single adsorbed alkali ion can affect the IR spectra of up to 27 coadsorbed CO molecules [37].

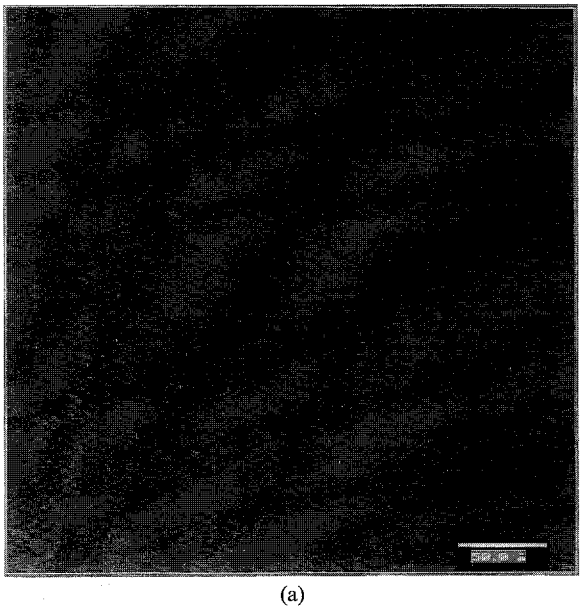

(a)

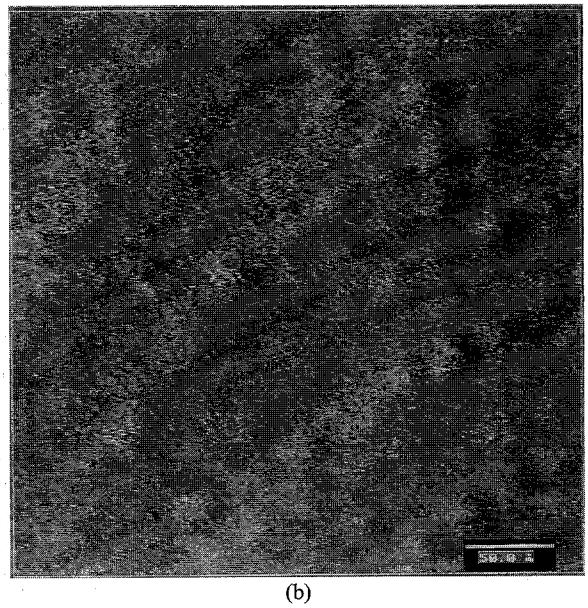

(b)

Fig. 2. STM images (unfiltered) of the (a) sodium-cleaned and (b) sodium-dosed Pt(111)-(2 × 2)-O adlattice showing the reversible appearance of the Pt(111)-(12 × 12)-Na adlayer ($V_t = +100$ mV, $I_t = 1.8$ nA, total scan size 319 Å).

The Pt(111)-(12 × 12)-Na adlattice on the

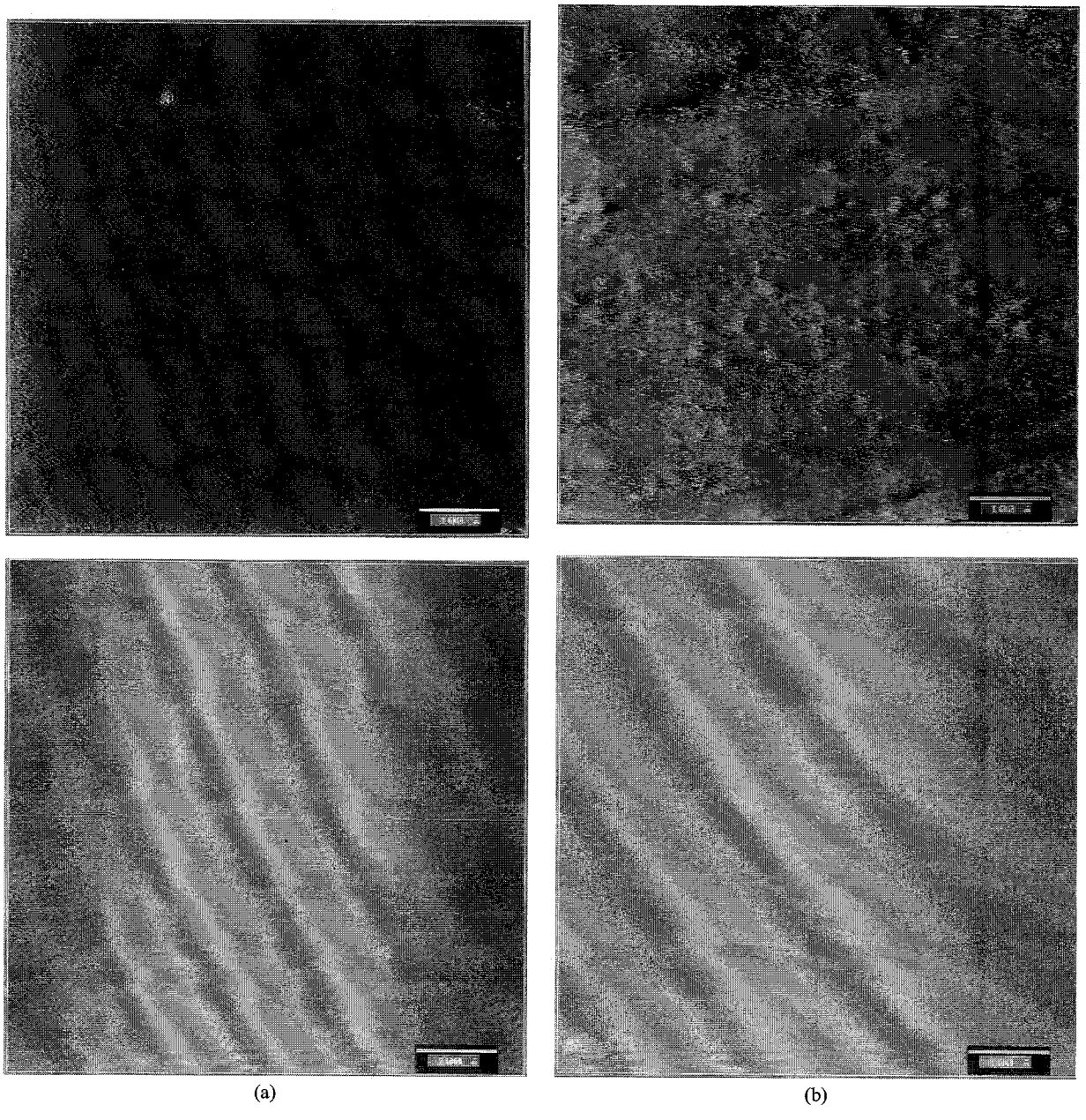

(a) (b)

Fig. 3. STM images (unfiltered) and corresponding Fourier spectra of the (a) sodium-cleaned and (b) sodium dosed Pt(111)-(2×2)-O adlattice. Total scan size 638 Å, other conditions as in Fig. 2.

sodium-doped surface is present over atomically enormous domains of the Pt(111) surface, as shown in Fig. 5. We could find no patches of the Pt(111) surface not covered by the Pt(111)-(12×12)-Na adlattice.

4. Discussion

The electrochemically induced creation of the Pt(111)-(12×12)-Na adlayer, manifest by STM at low Na coverages, is strongly corroborated by the

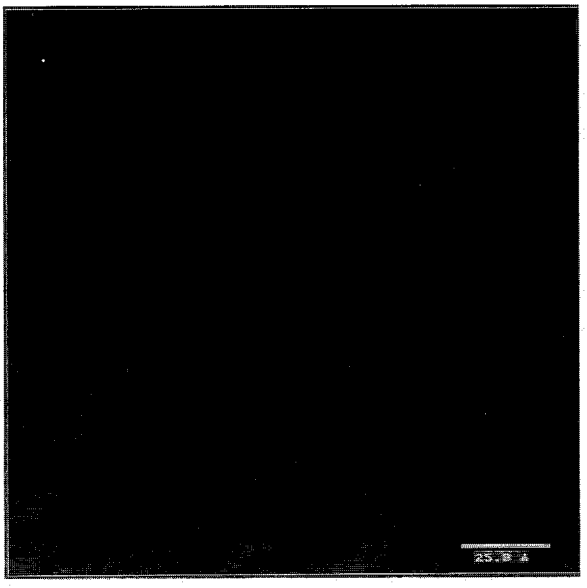

(a)

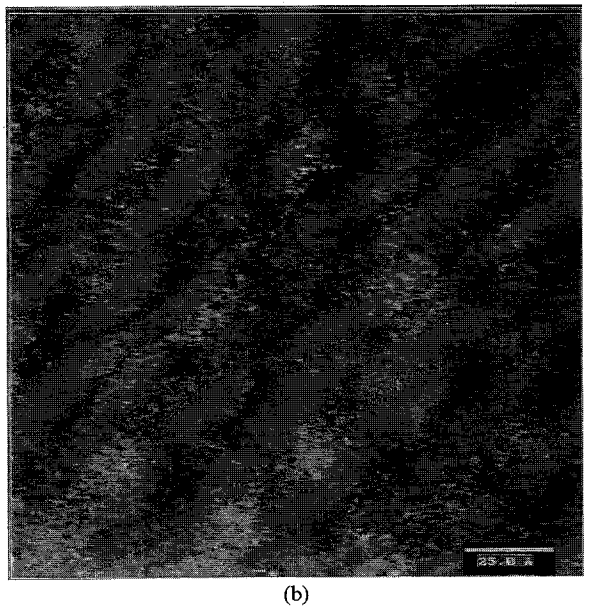

(b)

Fig. 4. Low scanning-area STM images (unfiltered) of the (a) sodium-cleaned and (b) sodium-dosed Pt(111)-(2×2)-O adlattice. Total scan size 159 Å, other conditions as in Fig. 2.

corresponding catalyst potential V_{WR} and work function $e\Phi$ response to galvanostatic transients in electrochemical promotion experiments utilizing polycrystalline Pt films exposed to air and deposited on β''-Al_2O_3 [22,38]. Previous exploratory STM studies have shown that the surface of these films is largely composed of low Miller-index Pt(111) planes [24].

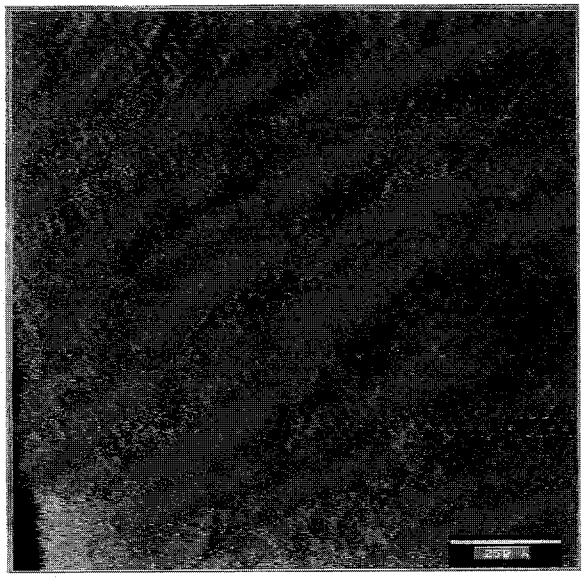

Fig. 5. Large scanning-area STM image (unfiltered) of the Pt(111)-(12×12)-Na adlattice. $V_t=500$ mV, $I_t=2.5$ nA, total scan size 1275 Å.

Two examples of the observed V_{WR} variation with sodium coverage on the Pt catalyst surface are shown in Fig. 6, together with the concomitant variation in the rates of CO [22] and C_2H_4 [38] oxidation. In these experiments the Na coverage θ^{O}_{Na} was varied via galvanostatic negative current application, corresponding to the supply of $(-It/F)$mol Na onto the Pt catalysts of measured maximum reactive oxygen uptake (N mol of O). Consequently, the resulting Na coverage θ^{O}_{Na}, based on the maximum number of surface oxygen atoms, can be computed from [22,38]

$$\theta^{O}_{Na}=-It/FN. \quad (1)$$

Assuming that the reactive oxygen corresponds to the oxygen which forms the well-known Pt(111)-(2×2)-O structure [39], one can define the second Na coverage scale, θ^{Pt}_{Na}, shown in Fig. 6, which is based on the number of surface Pt atoms, and equals

$$\theta^{Pt}_{Na}=(0.25)\theta^{O}_{Na}. \quad (2)$$

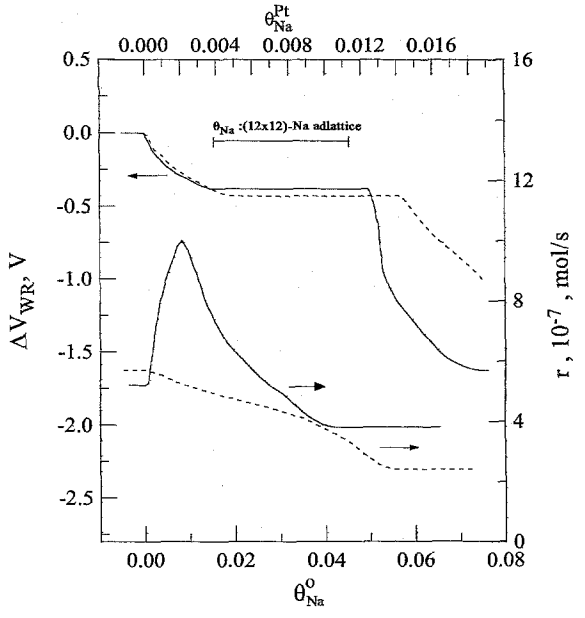

Fig. 6. Effect of sodium coverage on the change ΔV_{WR} of polycrystalline Pt catalyst potential V_{WR} and on the catalytic rates of CO oxidation (solid lines, Ref. [38]) and C_2H_4 oxidation (dashed lines, Ref. [36]). Comparison with the theoretical Na coverage required to form the Pt(111)-(12 × 12)-Na adlayer; θ^{Pt}_{Na} is based on the number of surface Pt atoms; θ^{O}_{Na} is based on the number of surface O atoms corresponding to the Pt(111)-(2 × 2)-O adlattice. See text for discussion.

As shown in Fig. 6, increasing sodium coverage initially causes ($\theta^{O}_{Na} < 0.015$) a decrease in catalyst potential V_{WR} (and thus [21–24] work function $e\Phi$) followed by a rather wide sodium coverage region $\Delta\theta^{O}_{Na} \approx (0.035)$ where V_{WR} remains practically constant. The constancy of ΔV_{WR} with changing Na coverage strongly indicates the formation of an ordered structure whose chemical potential is independent of coverage. The osberved $\Delta\theta^{O}_{Na}$ and $\Delta\theta^{Pt}_{Na}$ values over which V_{WR} remains constant (0.035 and 0.00875, respectively) are in excellent agreement with the corresponding theoretical geometric Na coverages ($\Delta\theta^{O}_{Na} = 1/36 = 0.0278$, $\Delta\theta^{Pt}_{Na} = 1/144 = 0.00695$) required to form the Pt(111)-(12 × 12)-Na adlattice (Fig. 6).

It is worth noting that for both systems, the observed ΔV_{WR} value corresponding to the onset of the formation of the ordered Na adlattice is practically the same, which strongly supports the idea that this ΔV_{WR} value is characteristic of the chemical potential of this structure. The fact that a small but not negligible Na coverage ($\theta^{O}_{Na} < 0.015$) preceeds the formation of the ordered Na structure on the surface of polycrystalline Pt samples (Fig. 6) may indicate preferential Na adsorption on stepped surfaces before Na adsorption on Pt(111) starts taking place.

It should be noted that in the present study Na back-spillover takes place not only on the surface of the Pt(111) single crystal (surface area 1 cm^2, thus 1.53×10^{15} surface Pt atoms or 2.54×10^{-9} surface Pt mol) but also on the surface of the connecting porous Pt film along the perimeter of the Pt(111) monocrystal. Therefore only a small fraction (1.76×10^{-11} mol Na, i.e. roughly 0.12% of the totally supplied Na) creates the (12 × 12)-Na adlayer on the single-crystal surface, and the rest is used to establish an equivalent Na coverage on the connecting porous Pt film of surface area ~800 cm^2. It is worth emphasizing that the change $\Delta V_{WR} = -1$ V in the Pt(111) catalyst potential during electrochemical Na supply measured in the present work and the concomitant [21,24] decrease of 1 eV in the work function of the Pt(111) surface is consistent, in view of Fig. 6, with the completion of the (12 × 12)-Na adlattice, i.e. with a θ^{O}_{Na} value in excess of 0.05.

As previously noted the constancy of catalyst potential V_{WR} during the formation of the Pt-(12 × 12)-Na adlayer, followed by a rapid decrease in catalyst potential and work function when more Na is forced to adsorb on the surface (Fig. 6), is thermodynamically consistent with the formation of an ordered layer whose chemical potential is independent of coverage. A systematic study of the temperature dependence of V_{WR} may allow for the estimation of the enthalpy and entropy of this ordered adlayer.

The formation of the ordered Pt-(12 × 12)-Na structure over the entire Pt(111) surface shows that the repulsive dipole–dipole interactions of the partly ionized Na atoms (which are accompanied by their image charges in the metal [21,24]) overbalances the attractive Madelung-type attraction between the Na adlayer and the underlying (2 × 2)-O adlattice. This is corroborated by the fact that the catalytic rate relaxation time constant τ during galvanostatic transients in electrochemical

promotion studies utilizing Pt/Na-β''-Al_2O_3 has been found to be given by [24]

$$\tau = FN\theta^{o}_{Na}/I, \quad (3)$$

where N is the catalyst surface area expressed in mol adsorbed O. Eq. (3) strongly suggests that electrochemically supplied Na spreads uniformly everywhere on the gas-exposed catalyst surface due to the dominating repulsive dipole–dipole interactions of Na adatoms.

5. Conclusions

The present STM results show that:

(1) Spillover–back-spillover phenomena can take place over enormous (~mm) atomic distances.
(2) Electrochemically induced and controlled Na back-spillover is the origin of electrochemical promotion on Pt when using Na-β''-Al_2O_3 solid electrolytes.
(3) Promoters can form ordered structures on catalyst surfaces under ambient conditions relevant to industrial practice.

The use of STM to image promoters and to study spillover and back-spillover phenomena on catalyst surfaces under atmospheric pressure conditions relevant to industrial catalysis is a valuable tool for studying promotional phenomena at the molecular level.

Acknowledgements

We thank EPRI, the CEC JOULE Programme, the Hellenic Secretariat of Research of Technology and the INTAS Programme for financial support, and Professor R.M. Lambert for numerous helpful discussions.

References

[1] G. Binnig and H. Rohrer, Surf. Sci. 126 (1983) 236.
[2] F. Ogletree and M. Salmeron, Prog. Solid State Chem. 20 (1990) 235.
[3] P. Avouris, J. Phys. Chem. 94 (1990) 2246.
[4] W. Weiss, U. Starke and G.A. Somorjai, Anal. Chim. Acta 297 (1994) 109.
[5] W. Haiss, D. Lackey, J.K. Sass and K.H. Besocke, J. Chem. Phys. 95 (1991) 2193.
[6] R. Sonnenfeld and P.K. Hansma, Science 232 (1986) 211.
[7] A.J. Arvia and R.C. Salvarezza, Electrochim. Acta 11/12 (1994) 1481.
[8] R.J. Nichols, O.M. Magnussen, J. Hotlus, T. Twomey, R.J. Behm and D.M. Kolb, J. Electroanal. Chem. 290 (1990) 21.
[9] R. Sonnenfeld, J. Schneir and P.K. Hansma, in: Modern Aspects of Electrochemistry, Vol. 21, Eds. R.E. White and J.O'.M. Bockris (Plenum, New York, 1990) pp. 1–28.
[10] C.M. Vitus, S.-C. Chiang, B.C. Schardt and M.J. Weaver, J. Phys. Chem. 95 (1991) 7559.
[11] R.Q. Hwang, D.M. Zeglinsky, D.E. Ogletree, A.L. Vazquez-de-Parga, G.A. Somorjai and M. Salmeron, Phys. Rev. B 44 (1991) 1914.
[12] C.J. Chen, Introduction to Scanning Tunneling Microscopy (Oxford University Press, Oxford, 1993), and references therein.
[13] J.V. Barth, R.J. Behm and G. Ertl, Surf. Sci. 341 (1995) 62.
[14] B.J. McIntyre, M.B. Salmeron and G.A. Somorjai, Catal. Lett. 14 (1992) 263.
[15] M. Boudart and G. Djega-Mariadassou, in: Kinetics of Heterogeneous Catalytic Reactions (Princeton University Press, Princeton, NJ, 1984).
[16] B. Grzybowska-Swierkosz and J. Haber, in: Annual Reports on the Progress of Chemistry, Vol. 91 (The Royal Society of Chemistry, Cambridge, 1994) pp. 395–439.
[17] M.P. Kiskinova, in: Poisoning and Promotion in Catalysis based on Surface Science Concepts and Experiments (Elsevier, Amsterdam, 1992).
[18] H.P. Bonzel, Surf. Sci. Rep. 8 (1987) 43–125.
[19] B. Delmon in: New Aspects of Spillover Effect in Catalysis, Eds. T. Inui, K. Fujimoto, T. Uchijima and M. Masai (Elsevier, Amsterdam 1993) pp. 1–9.
S.J. Teichner, in: New Aspects of Spillover Effect in Catalysis, Eds. T. Inui, K. Fujimoto, T. Uchijima and M. Masai (Elsevier, Amsterdam, 1993) pp. 27–45.
[20] S. Ladas, S. Kennou, S. Bebelis and C.G. Vayenas, J. Phys. Chem. 97 (1993) 8845.
[21] C.G. Vayenas, S. Bebelis and S. Ladas, Nature (London) 343 (1990) 625.
[22] I.V. Yentekakis, G. Moggridge, C.G. Vayenas and R.M. Lambert, J. Catal. 146 (1994) 292.
[23] S. Neophytides, D. Tsiplakides, P. Stonehart, M.M. Jaksic and C.G. Vayenas, Nature (London) 370 (1994) 45.
[24] C.G. Vayenas, M.M. Jaksic, S. Bebelis and S. Neophytides, in: Modern Aspects of Electrochemistry, Vol. 29, Eds. J.O'.M. Bockris, B.E. Conway and R.E. White (Plenum, New York, 1995) pp. 57–202, and references therein.
[25] C. Pliangos, I.V. Yentekakis, X.E. Verykios and C.G. Vayenas, J. Catal. 154 (1995) 124.
[26] I.R. Harkness and R.M. Lambert, J. Catal. 152 (1995) 211.
[27] J.O.'M. Bockris and Z. Minevski, Electrochim. Acta 39 (1994) 1471.

[28] S. Ladas, S. Bebelis and C.G. Vayenas, Surf. Sci. 251/252 (1991) 1062.
[29] C.A. Cavalca, PhD Thesis, Yale University, 1996.
[30] W. Zipprich, H.-D. Wiemhöfer, U. Vöhrer and W. Göpel, Ber. Bunsenges. Phys. Chem. 99 (1995) 1406.
[31] D.I. Kondarides, G.N. Papatheodorou, C.G. Vayenas and X.E. Verykios, Ber. Bunsenges. Phys. Chem. 97 (1993) 709.
[32] L. Basini, C.A. Cavalca and G.L. Haller, J. Phys. Chem. 98 (1994) 10853.
[33] S. Neophytides and C.G. Vayenas, J. Phys. Chem. 99 (1995) 17063.
[34] C. Cavalca, G. Larsen, C.G. Vayenas and G.L. Haller, J. Phys. Chem. 97 (1993) 6115.
[35] G. Pacchioni, F. Illas, S. Neophytides and C.G. Vayenas, J. Phys. Chem., in press.
[36] K.H. Besocke, Surf. Sci. 181 (1987) 145.
[37] K.J. Uram, L. Ng and J.T. Yates, Jr., Surf. Sci. 177 (1986) 253.
[38] C.G. Vayenas, S. Bebelis and M. Despotopoulou, J. Catal. 128 (1991) 415.
[39] C.T. Campbell, G. Ertl, H. Kuipers and J. Segner, Surf. Sci. 107 (1981) 220.